4. Hentschel, M. *et al.* Attosecond metrology. *Nature* **414,** 509–513 (2001).
5. Kienberger, R. *et al.* Atomic transient recorder. *Nature* **427,** 817–821 (2004).
6. Tzallas, P., Charalambidis, D., Papadogiannis, N. A., Witte, K. & Tsakiris, G. D. Direct observation of attosecond light bunching. *Nature* **426,** 267–271 (2003).
7. Kondo, K., Tamida, T., Nabekawa, Y. & Watanabe, S. High-order harmonic generation and ionization using ultrashort KrF and Ti:sapphire lasers. *Phys. Rev. A.* **49,** 3881–3889 (1994).
8. Christov, I. P., Murnane, M. M. & Kapteyn, H. C. Generation and propagation of attosecond x-ray pulses in gaseous media. *Phys. Rev. A.* **57,** R2285–R2288 (1998).
9. Agostini, P., Fabre, F., Mainfray, G., Petite, G. & Rahman, N. K. Free–free transitions following six-photon ionization of xenon atoms. *Phys. Rev. Lett.* **42,** 1127–1130 (1979).
10. Nikolopoulos, L. A. A. & Lambropoulos, P. Multichannel theory of two-photon single and double ionization of helium. *J. Phys. B* **34,** 545–564 (2001).
11. Kobayashi, Y., Sekikawa, T., Nabekawa, Y. & Watanabe, S. 27-fs extreme ultraviolet pulse generation by high-order harmonics. *Opt. Lett.* **23,** 64–66 (1998).
12. Sekikawa, T., Ohno, T., Yamazaki, T., Nabekawa, Y. & Watanabe, S. Pulse compression of a high-order harmonic by compensating the atomic dipole phase. *Phys. Rev. Lett.* **83,** 2564–2567 (1999).
13. Sekikawa, T., Katsura, T., Miura, S. & Watanabe, S. Measurement of the intensity-dependent atomic dipole phase of a high harmonic by frequency-resolved optical gating. *Phys. Rev. Lett.* **88,** 193902 (2002).
14. Diels, J.-C. & Rudolph, W. *Ultrashort Laser Pulse Phenomena* (Academic, San Diego, 1996).
15. Christov, I. P., Murnane, M. M. & Kapteyn, H. C. High-harmonic generation of attosecond pulses in 'single-cycle' regime. *Phys. Rev. Lett.* **78,** 1251–1254 (1997).
16. Sekikawa, T., Kanai, T. & Watanabe, S. Frequency-resolved optical gating of femtosecond pulses in the extreme ultraviolet. *Phys. Rev. Lett.* **91,** 103902 (2003).
17. Becker, W., Long, S. & McIver, J. K. Modeling harmonic generation by a zero-range potential. *Phys. Rev. A.* **50,** 1540–1560 (1994).
18. Ammosov, M. V., Delone, N. B. & Krainov, V. P. Tunnel ionization of complex atoms and of atomic ions in an alternating electromagnetic field. *Sov. Phys. JETP* **64,** 1191–1194 (1986).
19. Antoine, P. *et al.* Generation of attosecond pulses in macroscopic media. *Phys. Rev. A.* **56,** 4960–4969 (1997).
20. Kanai, T., Zhou, X., Sekikawa, T., Watanabe, S. & Togashi, T. Generation of sub-TW, sub-10 fs violet pulses at 1–5 kHz by broadband frequency doubling. *Opt. Lett.* **28,** 1484–1486 (2003).
21. Nabekawa, Y., Kuramoto, Y., Togashi, T., Sekikawa, T. & Watanabe, S. Generation of 0.66-TW pulses at 1 kHz by a Ti:sapphire laser. *Opt. Lett.* **23,** 1384–1386 (1998).
22. Itatani, J. *et al.* Attosecond streak camera. *Phys. Rev. Lett.* **88,** 173903 (2002).
23. Trebino, R. *et al.* Measuring ultrashort laser pulses in the time-frequency domain using frequency-resolved optical gating. *Rev. Sci. Instrum.* **68,** 3277–3295 (1997).
24. Barty, C. P. J. *et al.* Regenerative pulse shaping and amplification of ultrabroadband optical pulses. *Opt. Lett.* **21,** 219–221 (1996).

Acknowledgements This work was supported by the Ministry of Education, Culture, Sports, Science and Technology of Japan.

Competing interests statement The authors declare that they have no competing financial interests.

Correspondence and requests for materials should be addressed to S.W. (watanabe@issp.u-tokyo.ac.jp).

Large fluctuations in speed on Greenland's Jakobshavn Isbræ glacier

Ian Joughin[1]*, Waleed Abdalati[2] & Mark Fahnestock[3]

[1]*Jet Propulsion Lab, California Institute of Technology, USA*
[2]*NASA Goddard Space Flight Center, Oceans and Ice Branch, Code 971, Greenbelt, Maryland 20771, USA*
[3]*Complex Systems Research Center, Institute for the Study of Earth, Oceans and Space, University of New Hampshire, Durham, New Hampshire 03824, USA*

* Present address: Polar Science Center, Applied Physics Laboratory, University of Washington, 1013 NE 40th Street, Seattle, Washington, 9810-6698, USA

It is important to understand recent changes in the velocity of Greenland glaciers because the mass balance of the Greenland Ice Sheet is partly determined by the flow rates of these outlets. Jakobshavn Isbræ is Greenland's largest outlet glacier[1], draining about 6.5 per cent of the ice-sheet area, and it has been surveyed repeatedly since 1991 (ref. 2). Here we use remote sensing data to measure the velocity of Jakobshavn Isbræ between 1992 and 2003. We detect large variability of the velocity over time, including a slowing down from 6,700 m yr^{-1} in 1985 to 5,700 m s^{-1} in 1992, and a subsequent speeding up to 9,400 m yr^{-1} by 2000 and 12,600 m yr^{-1} in 2003. These changes are consistent with earlier evidence for thickening of the glacier in the early 1990s and rapid thinning thereafter[3]. Our observations indicate that fast-flowing glaciers can significantly alter ice discharge at sub-decadal timescales, with at least a potential to respond rapidly to a changing climate.

Because of its contribution to the Greenland Ice Sheet's mass balance, an airborne laser altimeter has surveyed the Jakobshavn Isbræ glacier repeatedly since 1991 (ref. 2). When many other glaciers were thinning, these surveys revealed that Jakobshavn Isbræ thickened substantially from 1991 to 1997 (ref. 4) at elevations less than 1,100 m. After 1997, the glacier began thinning rapidly with peak rates of ~15 m yr^{-1} (ref. 3).

We used interferometric synthetic aperture radar (InSAR) to measure Jakobshavn Isbræ's velocity in 1992, 1994, 1995 and 2000 (ref. 5). We also applied feature-tracking methods to Landsat-image pairs to determine velocity in 2001, 2002 and 2003. Earlier velocity measurements were made using airborne imaging from the summer of 1985 (ref. 6) and by tracking crevasse displacements in laser-altimeter surveys from 1997 (ref. 7).

Figure 1 shows the 1992 and 2000 speeds, illustrating a large speed-up by 2000 that extends over much of the fast-moving region. This increase is also visible in plots of the glacier's centreline speed (Fig. 2). Inland of ~40 km, there is no appreciable change over the 18-yr period. Closer to the ice front, the 2000-to-2003 speeds increase steadily over time relative to the fairly stable mid-1990s. From 1985 to 1992, however, the glacier slowed just before observed thickening[3].

Figure 3 shows speeds on the fastest-moving (>5,000 m yr^{-1}) areas averaged at over 20 locations corresponding to the 1985 measurements[6] (Fig. 1, purple symbols) and at several hundred locations corresponding to measurements[7] made in 1997 (Fig. 1, orange line). The 1985 mean speed was 6700 m yr^{-1}, which in 1992 decreased to 5700 m yr^{-1} and remained nearly constant until 1997. Between May 1997 and October 2000, the glacier speed reached 9,400 m yr^{-1} and flowed at about this rate in May 2001. Over the next two months, the glacier speed increased to 10,000 m yr^{-1}. By summer 2002, the speed had increased to 11,900 m yr^{-1} and then to 12,600 m yr^{-1} in spring 2003, which is the last period for which we have velocities.

The mid-1990s slow interval corresponds well with the 1991-to-1997 measured thickening[3]. The 1985 calving rate was ~26.5 km^3 yr^{-1} (ref. 8), so the 1,000 m yr^{-1} drop in speed by 1992 suggests a discharge reduction of ~4 km^3 yr^{-1}. Most of the slowdown occurred over the region moving faster than 1,000 m yr^{-1}. If we assume thickening was confined to this fast-moving area, then we estimate an average thickening of ~1 m yr^{-1}, which is consistent with observed rates[3]. The 1985-to-2003 speed-up implies a near-doubling in discharge to 50 km^3 yr^{-1}. Excluding the former ice tongue's area, this implies an average thinning of ~6 m yr^{-1} over the fast-moving region, which is also consistent with observations[3]. Thus, the speed variations are sufficient to explain the observed elevation changes as dynamic thickening and thinning[3].

Meltwater input to the bed seasonally affects nearby inland ice speed[9], but these fluctuations are far smaller than the changes we observe. Although we have only coarse intra-annual sampling, our results suggest a trend of increasing speed starting after 1997, rather than a seasonal pattern of summer speed-up and winter slow-down[9]. The speed-up appears to persist through the winter, so it seems unlikely that increased surface-meltwater input to the bed directly caused the acceleration. Earlier observations that found no seasonal variation on Jakobshavn Isbræ[6,10] support this hypothesis, as does our analysis of 2001–2002 spring and summer Landsat data.

From 1850 to 1962 (ref. 11), the calving front retreated by ~26 km but stabilized and remained within a 2.5-km-long calving zone from 1962 to the 1990s[12]. In October 2000, this pattern changed when a progressive retreat began that resulted in nearly complete disintegration of the ice shelf by May 2003.

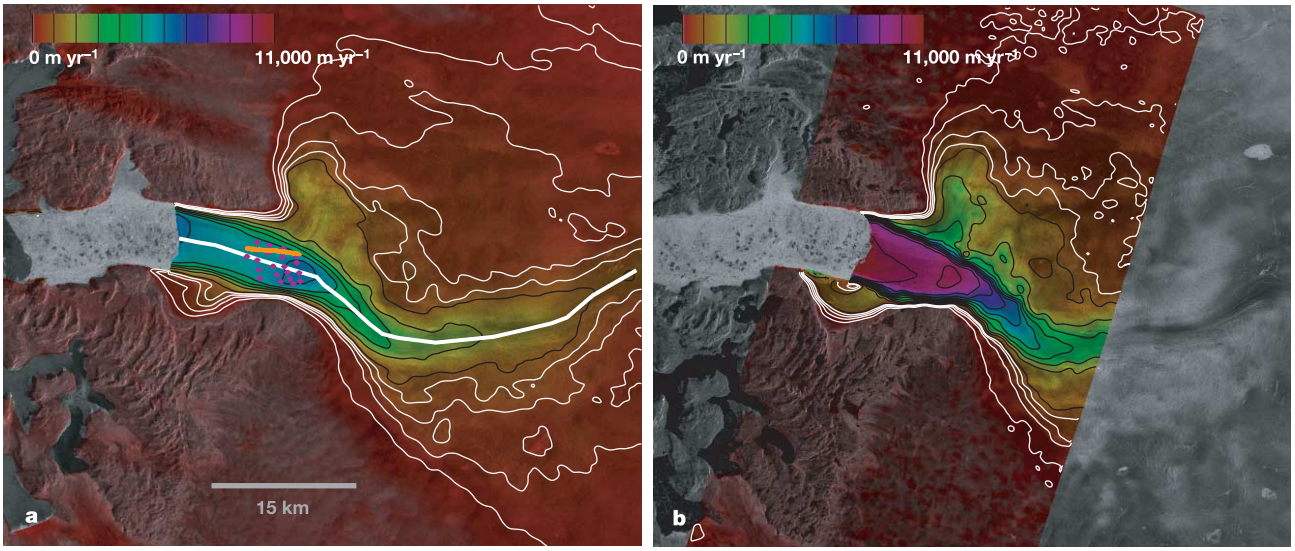

Figure 1 Ice-flow speed as colour over SAR amplitude imagery of Jakobshavn Isbræ in February 1992 (**a**) and October 2000 (**b**). In addition to colour, speed is contoured with thin black lines at 1,000 m yr^{-1} intervals and with thin white lines at 200, 400, 600 and 800 m yr^{-1}. The thick white line shows the location of the profile plotted in Fig. 2. The locations of velocity measurements made in 1997 (orange line) and 1985 (purple symbols) are also shown.

The calving front's multi-decadal stability has been attributed to resistance from the fjord walls and pinning points that may have yielded a restraining "back-stress" on the floating ice with an influence extending above the grounding zone[1,13]. Several of the speed increases coincide with losses of sections of the ice tongue as it broke up. Satellite images also indicate that several large rifts began developing in 2000 along the fjord's northern wall, which may have reduced lateral resistance. Thus, back-stress reduction from the ice tongue's disintegration may have caused or contributed to the speed-up. This is consistent with observations elsewhere of acceleration following ice shelf loss[14,15].

If the ice tongue's weakening and retreat caused the speed-up, then it is not clear what initiated the retreat after a period of multi-decadal stability[12]. At nearby Egedesminde, the 1998–2001 melt intensity was abnormally high[3] and passive microwave data indicate a high melt extent in 2002. Calving rates are higher in summer[12], indicating a sensitivity to temperature and melt[13,16,17]. Thus, increased calving may have forced the ice tongue to retreat beyond its stable position to initiate the acceleration.

Jakobshavn Isbræ's acceleration and near-doubling of ice discharge is noteworthy because this single glacier has increased the rate of sea-level rise by ~0.06 mm yr^{-1}, or ~4% of the 20th-century rate[18]. If the retreat of the ice tongue caused the acceleration, then similar losses of floating ice tongues since the Little Ice Age[11] may explain[13] the current rapid thinning observed for many of Greenland's outlet glaciers[4,19]. This speed-up is the most striking of several ice-stream and outlet-glacier speed-ups and slow-downs observed, with just over a decade of spaceborne InSAR measurements[20–23]. Collectively, these observations indicate that fast-flowing glaciers can significantly alter ice-sheet discharge at sub-decadal timescales and that their response to climate change has at least the potential to be rapid. This argues both for further investigation of ice-sheet mass balance and improved incorporation of fast flow features into ice-sheet models, many of which predict response times on the centurial-to-millennial scale[24]. □

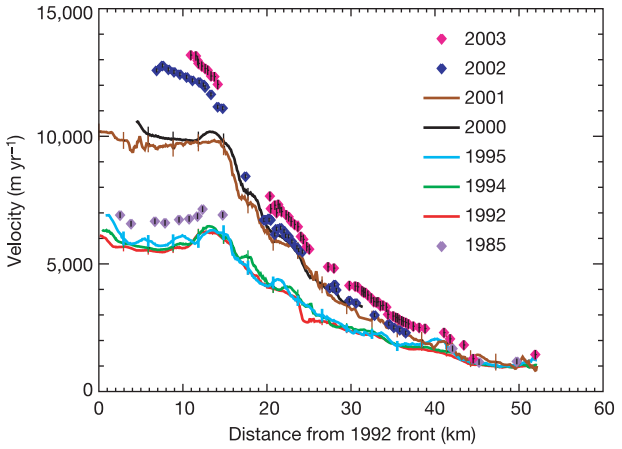

Figure 2 Profiles of speckle-tracked (see Methods), Landsat, airborne feature-tracked speed from along the line shown in Fig. 1a and as a function of distance from the approximate position of the 1992 calving front. One-sigma error bars are shown at several-kilometre intervals. The 1985 (ref. 6), 2002 and 2003 data sets were sparsely sampled, so only individual point measurements are plotted. The data were acquired over the periods from February to March 1992, December 1993 to March 1994, November 1995, October to November 2000, May 2001, July to September 2002, and March to May 2003.

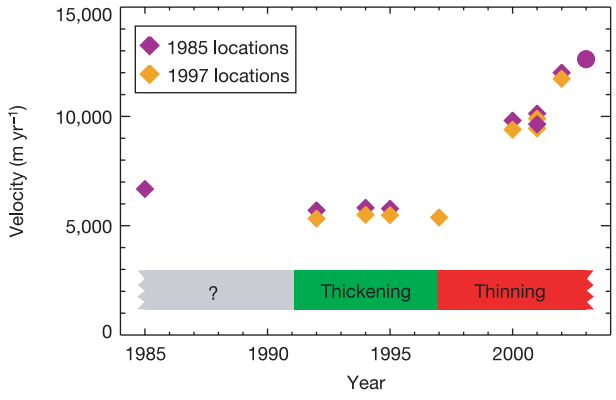

Figure 3 Average speeds versus time for measurements made at original 1985 and 1997 airborne survey locations (same-colour symbols in Fig. 1). For 2001, the slower two points are from a 4–20 May pair, whereas the faster points are from a 20 May to 7 July pair. Laser altimeter surveys determined the periods of thickening and thinning[3]. Minor speed differences for 1985 and 1997 locations reflect the different areas that were sampled. Because much of the floating ice tongue was missing in 2003, the speed for this year (circle) is an average of the points on the remaining ice.

Methods

A set of speckle-tracking algorithms[5] was used to determine the 1992, 1994, 1995 and 2000 velocities from 1–24-day image pairs. Speckle tracking uses the displacements of the correlated speckle patterns in pairs of SAR images to derive ice motion estimates. Individual errors were up to a few hundred metres per year (see Fig. 2), but errors on averages (for example, Fig. 3) are below 100 m yr^{-1}. We did not tide-correct the speckle-tracked data, so there are biases on the floating ice that do not spatially average out. To assess this error, we estimated velocity for five 1992 InSAR pairs, each with different tidal errors. The standard deviation for these estimates was 69 m yr^{-1}. Our 1992 and 1994 estimates are temporal averages of multiple (2 to 5) same-year pairs, which further reduces this error. The 2001 through 2003 estimates were derived using the IMCORR[25] feature-tracking software applied to 16-to-64-day Landsat image pairs. Established methods[26] were applied to passive microwave data to determine the 2002 melt extent.

Received 7 July; accepted 8 October 2004; doi:10.1038/nature03130.

1. Echelmeyer, K., Clarke, T. S. & Harrison, W. D. Surficial glaciology of Jakobshavns Isbrae, West Greenland. 1. Surface morphology. *J. Glaciol.* **37,** 368–382 (1991).
2. Krabill, W. *et al.* Greenland ice sheet: High-elevation balance and peripheral thinning. *Science* **289,** 428–430 (2000).
3. Thomas, R. H. *et al.* Investigation of surface melting and dynamic thinning on Jakobshavn Isbrae, Greenland. *J. Glaciol.* **49,** 231–239 (2003).
4. Abdalati, W. *et al.* Outlet glacier and margin elevation changes: Near-coastal thinning of the Greenland ice sheet. *J. Geophys. Res.* **106,** 33729–33741 (2001).
5. Joughin, I. Ice-sheet velocity mapping: a combined interferometric and speckle-tracking approach. *Ann. Glaciol.* **34,** 195–201 (2002).
6. Fastook, J. L., Brecher, H. H. & Hughes, T. J. Derived bedrock elevations, strain rates and stresses from measured surface elevations and velocities—Jakobshavns Isbrae, Greenland. *J. Glaciol.* **41,** 161–173 (1995).
7. Abdalati, W. & Krabill, W. B. Calculation of ice velocities in the Jakobshavn Isbrae area using airborne laser altimetry. *Remote Sens. Environ.* **67,** 194–204 (1999).
8. Echelmeyer, K., Harrison, W. D., Clarke, T. S. & Benson, C. Surficial glaciology of Jakobshavns Isbrae, West Greenland. 2. Ablation, accumulation and temperature. *J. Glaciol.* **38,** 169–181 (1992).
9. Zwally, H. J. *et al.* Surface melt-induced acceleration of Greenland ice-sheet flow. *Science* **297,** 218–222 (2002).
10. Echelmeyer, K. & Harrison, W. D. Jakobshavns Isbrae, West Greenland—Seasonal variations in velocity or lack thereof. *J. Glaciol.* **36,** 82–88 (1990).
11. Weidick, A. *Satellite Image Atlas of Glaciers of the World, Greenland* (USGS Professional Paper 1386-C, United States Government Printing Office, Washington, 1995).
12. Sohn, H. G., Jezek, K. C. & van der Veen, C. J. Jakobshavn Glacier, West Greenland: 30 years of spaceborne observations. *Geophys. Res. Lett.* **25,** 2699–2702 (1998).
13. Hughes, T. The Jakobshavns effect. *Geophys. Res. Lett.* **13,** 46–48 (1986).
14. Rott, H., Rack, W., Skvarca, P. & De Angelis, H. Northern Larsen Ice Shelf, Antarctica: further retreat after collapse. *Ann. Glaciol.* **34,** 277–282 (2002).
15. De Angelis, H. & Skvarca, P. Glacier surge after ice shelf collapse. *Science* **299,** 1560–1562 (2003).
16. Scambos, T. A., Hulbe, C., Fahnestock, M. & Bohlander, J. The link between climate warming and break-up of ice shelves in the Antarctic peninsula. *J. Glaciol.* **46,** 516–530 (2000).
17. van der Veen, C. J. Fracture mechanics approach to penetration of surface crevasses on glaciers. *Cold Regions Sci. Technol.* **27,** 31–47 (1998).
18. IPCC. *Climate Change 2001: Working Group I: The Scientific Basis* (eds Houghton, J. T. *et al.*) Ch. 11 ⟨http://www.grida.no/climate/ipcc_tar/wg1/index.htm⟩ (Intergovernmental Panel on Climate Change, Cambridge Univ. Press, Cambridge, 2001).
19. Thomas, R. H. *et al.* Substantial thinning of a major east Greenland outlet glacier. *Geophys. Res. Lett.* **27,** 1291–1294 (2000).
20. Rignot, E., Vaughan, D. G., Schmeltz, M., Dupont, T. & MacAyeal, D. Acceleration of Pine Island and Thwaites glaciers, West Antarctica. *Ann. Glaciol.* **34,** 189–194 (2002).
21. Mohr, J. J., Reeh, N. & Madsen, S. N. Three-dimensional glacial flow and surface elevation measured with radar interferometry. *Nature* **391,** 273–276 (1998).
22. Joughin, I., Tulaczyk, S., Fahnestock, M. & Kwok, R. A mini-surge on the Ryder Glacier, Greenland, observed by satellite radar interferometry. *Science* **274,** 228–230 (1996).
23. Joughin, I., Tulaczyk, S., Bindschadler, R. & Price, S. F. Changes in West Antarctic ice stream velocities: Observation and analysis. *J. Geophys. Res.* **107** (B11), 2289, doi:10.1029/2001JB001029 (2002).
24. Paterson, W. S. B. *The Physics of Glaciers* 3rd edn (Pergamon, Oxford, 1994).
25. Scambos, T. A., Dutkiewicz, M. J., Wilson, J. C. & Bindschadler, R. A. Application of image cross-correlation to the measurement of glacier velocity using satellite image data. *Remote Sens. Environ.* **42,** 177–186 (1992).
26. Abdalati, W. & Steffen, K. Greenland ice sheet melt extent: 1979–1999. *J. Geophys. Res.* **106,** 33983–33988 (2001).

Acknowledgements This work was supported by the Cryospheric Sciences Program of NASA's Earth Science Enterprise. I.J. performed his contribution at the Jet Propulsion Laboratory, California Institute of Technology, under contract with the National Aeronautics and Space Administration. We thank H. Brecher for the 1985 velocity data and B. Csatho, K. In Huh and S. Manizade for acquiring and orthorectifying the Landsat imagery. Radarsat data were provided by CSA through ASF and ERS SAR data were provided by ESA through the VECTRA project.

Author contributions All authors contributed equally to this work.

Competing interests statement The authors declare that they have no competing financial interests.

Correspondence and requests for materials should be addressed to I.J. (ian@apl.washington.edu).

Human contribution to the European heatwave of 2003

Peter A. Stott[1], D. A. Stone[2,3] & M. R. Allen[2]

[1]*Met Office, Hadley Centre for Climate Prediction and Research (Reading Unit), Meteorology Building, University of Reading, Reading RG6 6BB, UK*
[2]*Department of Physics, University of Oxford, Oxford OX1 3PU, UK*
[3]*Department of Zoology, University of Oxford, Oxford OX1 3PS, UK*

The summer of 2003 was probably the hottest in Europe since at latest AD 1500[1–4], and unusually large numbers of heat-related deaths were reported in France, Germany and Italy[5]. It is an ill-posed question whether the 2003 heatwave was caused, in a simple deterministic sense, by a modification of the external influences on climate—for example, increasing concentrations of greenhouse gases in the atmosphere—because almost any such weather event might have occurred by chance in an unmodified climate. However, it is possible to estimate by how much human activities may have increased the risk of the occurrence of such a heatwave[6–8]. Here we use this conceptual framework to estimate the contribution of human-induced increases in atmospheric concentrations of greenhouse gases and other pollutants to the risk of the occurrence of unusually high mean summer temperatures throughout a large region of continental Europe. Using a threshold for mean summer temperature that was exceeded in 2003, but in no other year since the start of the instrumental record in 1851, we estimate it is very likely (confidence level >90%)[9] that human influence has at least doubled the risk of a heatwave exceeding this threshold magnitude.

Temperatures near the Earth's surface are rising globally[10], and evidence is mounting that most of the warming observed in recent decades has been caused by increasing atmospheric concentrations of greenhouse gases[9,11,12]. Anthropogenic increases in annual-mean temperatures have also been detected on continental scales, in Europe, North America and other land regions[13–15]. We first investigate the origins of long-term changes in decadal-mean European summer (June–August) temperatures, determining the changes attributable to anthropogenic drivers of the climate system and changes attributable to natural drivers. We then estimate how the risk of mean June–August temperatures exceeding a particular extreme threshold in any individual summer has changed as a result of this anthropogenic interference in the climate system.

Over the course of the twentieth century, June–August temperatures in Europe exhibited an overall increase, and a distinctive temporal pattern of temperature change, including cooling in the 1950s and 1960s (Fig. 1). We focus on the region bounded by 10° W and 40° E and 30–50° N (Fig. 1 inset), this being one of the regions chosen in previous studies[13,16] to represent climatically coherent regions sufficiently large to exhibit climate change signals above the noise of natural internal variability. We use a pre-selected region in order to minimize any bias that could result from selecting our region already knowing where the most extreme temperatures occurred. Even in such a large domain, 2003 was the warmest summer on record. The history of temperature change averaged over this region is well reproduced by simulations of the HadCM3 climate model[17], even at the model's relatively low spatial resolution (3.75° longitude by 2.5° latitude), when driven with both anthropogenic and natural drivers of climate change (Fig. 1; see red, green, blue and turquoise lines). Four simulations (denoted ALL) were made with different initial conditions[18], each with the same combination of well mixed greenhouse gases, sulphate aerosols and changes in tropospheric and stratospheric ozone, as well as natural changes in solar output and explosive volcanic eruptions[12]. A calculation of the temperature changes due to natural drivers alone (obtained by combining a simulation with solar forcing and